



# A study of mechanism on infrared photoresponse in three-dimensional single-walled carbon nanotubes



Jongtaek Lee <sup>a</sup>, Taehee Park <sup>a</sup>, Jungwoo Lee <sup>a,1</sup>, Junyoung Lee <sup>a</sup>, Jonghee Yang <sup>a</sup>, Sang Jung Ahn <sup>a,b</sup>, Whikun Yi <sup>a,\*</sup>

<sup>a</sup> Research Institute for Natural Sciences and Department of Chemistry, Hanyang University, Seoul 133-791, South Korea

<sup>b</sup> Center for Advanced Instrumentation, Korea Research Institute of Standards and Science, Daejeon 34113, South Korea

## ARTICLE INFO

### Article history:

Received 21 April 2016

Received in revised form

10 June 2016

Accepted 18 June 2016

Available online 18 June 2016

## ABSTRACT

Two fundamental models have been formulated to explain the origin of the photoresponse in the electrical conductivity of SWNT films for an illumination of infrared (IR): the interband transition model (band model) and the bolometric model. However, the photoresponse of SWNTs has generated considerable debate, with various studies leading to different interpretations of the origin of photoconductivity. We fabricated three-dimensional SWNTs (3D-SWNTs) suspended between SiO<sub>2</sub> pillars grown on flat quartz to suggest the origin of the photoresponse of SWNTs. From the measurements of photoconductivity of our samples under three conditions using a continuous Xe lamp, one IR laser pulse, and a repeated IR laser pulse, we demonstrated that two response modes coexist.

© 2016 Published by Elsevier Ltd.

## 1. Introduction

Carbon nanotubes (CNTs) are considered to be promising building blocks for nanoelectronic and optical devices due to their unique geometry, high electrical conductivity, and exceptional mechanical and optical properties [1,2]. Optoelectronic materials that are responsive in the near-infrared (NIR) region (i.e., 800–2000 nm) are highly desirable for use in a number of demanding applications, including telecommunications, remote sensing, and solar cells [3]. Extensive effort has been devoted to elucidating the IR photoresponse in the electrical conductivity of individual single-walled carbon nanotubes (SWNTs) and SWNT films [4–8]. In particular, the photoresponse of pure CNT films and CNT/polymer composites has attracted tremendous attention because of their easy processability at macroscopic dimensions and potential application in optoelectronic devices [9,10]. Two fundamental models have been formulated to explain the origin of the photoresponse in the electrical conductivity of SWNT films: the

interband transition model (band model) and the bolometric model. However, the photoresponse of SWNTs has generated considerable debate, with various studies leading to different interpretations of the origin of photoconductivity.

In the band model, the photoresponse is attributed to the photoexcitation of electrons and holes, which enhances both the concentration of free carriers and the transport properties of a sensitive element [7,11]. However, some studies suggest that electron-hole pairs are strongly coupled in the one-dimensional SWNT crystal lattice, and that excitons rather than free carriers are the major product of photoexcitation [5,12–14]. In the bolometric model [8], electron-phonon interactions lead to ultrafast relaxation of photoexcited carriers, and the energy of incident IR irradiation is efficiently transferred to the crystal lattice of the sensing element, thereby heating the SWNT network. For prototype configurations based on SWNT bundles and films, the origin of photoconductivity was suggested to be bolometric in nature. In contrast, when SWNT-polymer composites [10] or only a few SWNTs [15] are utilized as sensitive materials, the origin of the photoresponse is predominantly attributed to the band model. It is known that SWNTs can be strongly affected by intertube junctions in the interior of the film or by the substrate through thermal contact. To prevent or minimize the effects of intertube junctions and the substrate, we fabricated three-dimensional SWNTs (3D-

\* Corresponding author. Tel.: +82 2 2220 0931; fax: +82 2 2298 0319.

E-mail address: [wkyi@hanyang.ac.kr](mailto:wkyi@hanyang.ac.kr) (W. Yi).

<sup>1</sup> Present address: National Research Foundation of Korea, 25, Heolleung-ro, seocho-gu, Seoul, Korea.

SWNTs) suspended between SiO<sub>2</sub> pillars grown on flat quartz (Fig. 1(a)). A scanning electron microscope (SEM) image of the structure is shown in Fig. 1(b). In this work, we measure the IR photoresponse of SWNTs under each condition, such as a continuous IR beam using Xe lamp (1), one IR laser pulse (pulse width of 5 ns, 2), and repeated IR laser pulses for 60 s (3) and report that two models coexist but only one model looks to be valid under specific circumstances.

## 2. Experimental

### 2.1. Formation of SiO<sub>2</sub> pillars

The SiO<sub>2</sub> pillar array was fabricated on a quartz (SiO<sub>2</sub>) substrate using an Oxford etcher. The SiO<sub>2</sub> substrate was patterned by a standard photolithography technique using a patterned chrome mask and reactive-ion etching in a CHF<sub>3</sub>/Ar gas mixture. After etching, any remaining patterned materials were stripped away, and the SiO<sub>2</sub> pillar substrate was subsequently cleaned by washing in acetone and alcohol. The diameter and height of the as-prepared SiO<sub>2</sub> pillars are 2.0 and 1.0 μm, respectively, while the Au comb electrodes (Fig. 1(c)) are 1.5 mm in width with a 300 μm spacing between the combs. Three pairs of anode and cathode electrodes made up a single sensor with an area of 4.2 mm<sup>2</sup>, which would be composed of 10 million SWNTs by comparing the surface area of unit pillar (8.14 μm<sup>2</sup>) and the number of SWNTs on the pillar to be 20 from the SEM picture. The size, shape and arrangement of the tubes could modify the dynamical response of photoconductivity, however, our photoresponse results showed similar trends within a 3% error.

### 2.2. Formation of 3D-SWNTs suspended on SiO<sub>2</sub> pillars

To form 3D-SWNT networks suspended on SiO<sub>2</sub> pillar arrays, a metal catalyst layer composed of 15 nm Al and 1 nm Fe particles was deposited on the SiO<sub>2</sub> pillar substrates by magnetron sputtering. The substrates were then placed on a sample holder in a thermal chemical vapor deposition (CVD) furnace, which was heated to 400 °C and maintained at that temperature for 15 min at  $1.0 \times 10^{-3}$  Torr in order to remove chemical residue from the specimens. The reactor was subsequently heated to 780 °C, and a 300 sccm flow of NH<sub>3</sub> gas (process gas) was injected into the reactor for 10 min to reduce the iron oxide catalyst. After the NH<sub>3</sub> pre-treatment, the temperature of the reactor was brought to 800 °C, and a 20 sccm flow of C<sub>2</sub>H<sub>2</sub> gas (carbon source gas) was injected to synthesize the SWNTs; the pressure inside the reactor was maintained at  $2.1 \times 10^{-1}$  Torr during this procedure. Finally, the CVD reactor was cooled down to room temperature in an N<sub>2</sub> environment.

### 2.3. Photocurrent measurements of the 3D-SWNTs suspended on SiO<sub>2</sub> pillars

The electrodes of the samples were composed of Cr (100 nm)/Au (100 nm) and were deposited on the surface of SWNT networks suspended on SiO<sub>2</sub> pillar substrates via magnetron sputtering; the distance between the two electrodes was 300 μm. The IR photoresponse of the SWNTs was measured under a voltage applied from a Keithley 2400 source meter in a continuous-flow cryostat. To evaluate the pressure and temperature dependence of the photoresponse, samples were evacuated in a cryostat and cooled by liquid N<sub>2</sub> vapor in the temperature range of 80 K to room

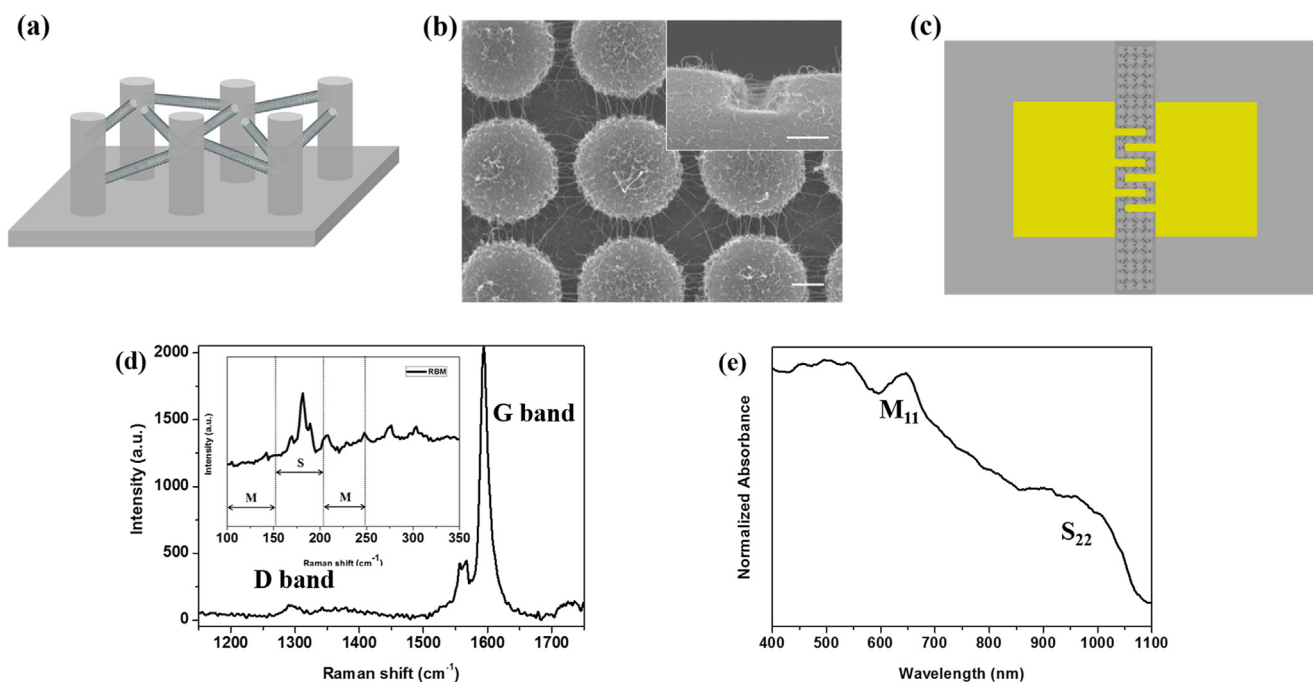


**Fig. 1.** (a) Schematic diagram of 3D-SWNTs suspended between SiO<sub>2</sub> pillars. (b) SEM image of the structure in (a); the scale bar is equal to 1 μm (inset: cross-sectional SEM image). (c) Au electrode configuration for the structure in (a). (d) Raman spectrum acquired for the 3D-SWNTs. (e) Absorption spectrum of the sample in a. Peaks in the absorption spectrum are observed at the second lowest energy semiconductor transition (S<sub>22</sub> around 1.23 eV) and the lowest energy metallic transition (M<sub>11</sub> around 1.90 eV). (A color version of this figure can be viewed online.)

Download English Version:

<https://daneshyari.com/en/article/1413144>

Download Persian Version:

<https://daneshyari.com/article/1413144>

[Daneshyari.com](https://daneshyari.com)